

## High-pressure studies on ferrites\*

N. A. Halasa, G. DePasquali, and H. G. Drickamer

*Department of Physics, School of Chemical Sciences, and Materials Research Laboratory, University of Illinois, Urbana, Illinois 61801*

(Received 10 December 1973)

High-pressure studies to 150 kbar have been made on four orthoferrites, on  $\text{NiFe}_2\text{O}_4$ , and on  $\text{Fe}_3\text{O}_4$  using Mössbauer resonance. For the last two compounds data were obtained at both 22 and 147 °C. The major features observed for the four rare-earth orthoferrites include an increase in the magnetic field with pressure which can be interpreted in terms of an increase in  $T_c$  with pressure, and a modest change in the quadrupole splitting, which depends on the size of the rare-earth ion. For  $\text{NiFe}_2\text{O}_4$  the changes in the magnetic field with pressure and temperature were complex and could best be interpreted in terms of a decrease in the saturation field  $H_0$  with pressure.  $H_0$  decreases more rapidly for the tetrahedral than for the octahedral site. For  $\text{Fe}_3\text{O}_4$ , with one tetrahedral and two octahedral sites, the behavior of the magnetic field at the tetrahedral site and that of the average value for the two octahedral sites is qualitatively similar to  $\text{NiFe}_2\text{O}_4$ . At 1 atm and 22 °C the isomer shifts at the two octahedral sites in  $\text{Fe}_3\text{O}_4$  are measurably different; however, by 40 kbar these isomer shifts become identical. At 147 °C and 1 atm there is a small difference in isomer shift between the two octahedral sites which disappears at modest pressure. These observations can be interpreted in terms of the rate of electron exchange between the sites.

### I. INTRODUCTION

The effect of pressure to 150 kbar has been measured on a series of ferrites using Mössbauer resonance to relate compression to changes in hyperfine interaction. The compounds studied include four rare-earth orthoferrites,  $\text{NiFe}_2\text{O}_4$ , and  $\text{Fe}_3\text{O}_4$  (magnetite).

The compounds were synthesized using  $\text{Fe}_2\text{O}_3$  enriched to 90% in  $^{57}\text{Fe}$ . The orthoferrites  $\text{LaFeO}_3$ ,  $\text{GdFe}_3$ , and  $\text{TmFeO}_3$  were prepared by mixing 30 mg of  $\text{Fe}_2\text{O}_3$  with stoichiometric amounts of  $\text{La}_2\text{O}_3$ ,  $\text{Gd}_2\text{O}_3$ , and  $\text{Tm}_2\text{O}_3$ , respectively. In synthesizing  $\text{PrFeO}_3$ , 30 mg of  $\text{Fe}_2\text{O}_3$  were mixed with enough  $\text{PrO}_2$  to give a one-to-one ratio of Fe and Pr. The oxide mixtures were pressed into pellets and pre-fired for 2 h at 900 °C in air and then reground and fired for 16 h at 1350 °C in air. The product was then slowly cooled. A Mössbauer spectrum of the product was obtained at room temperature and atmospheric pressure in order to ascertain that a single six-line magnetic spectrum was observed and that the parameters agreed with the published values.<sup>1</sup>

The nickel ferrite,  $\text{NiFe}_2\text{O}_4$ , was synthesized using normal ceramic techniques. A solution of  $\text{Ni}(\text{NO}_3)_2$  and  $\text{Fe}(\text{NO}_3)_3$  was prepared with the iron concentration twice that of the nickel. This solution was evaporated to dryness and heated to 400 °C in order to decompose the nitrate. The result was a mixture of  $\text{NiO}$  and  $\text{Fe}_2\text{O}_3$ . The powder was heated to 1125 °C in air for 4 h. This was slowly cooled and reground. The powder was heated to 1250 °C in air for 12 h and slowly cooled. The atmospheric-pressure Mössbauer spectrum of the product gave the expected hyperfine pattern.<sup>2</sup>

The magnetite,  $\text{Fe}_3\text{O}_4$ , was prepared by heating 50 mg of  $\text{Fe}_2\text{O}_3$  powder in a nitrogen atmosphere at 1400 °C for 12 h and slowly cooling the product. The atmospheric-pressure Mössbauer spectrum of the product gave a hyperfine pattern similar to published spectra.<sup>3,4</sup>

The high-pressure Mössbauer-resonance techniques have been previously described.<sup>5</sup> In this case, however, the multichannel analyzer was operated in the time mode, and the two halves of the readout were folded together to give a linear background. The spectra were fit with Lorentzian peaks, assuming equal  $f$  numbers at the different sites. The details of the fitting appear elsewhere.<sup>6</sup> At least three high-pressure runs (encompassing 5–6 pressures each) were made for each compound at 22 °C. Some data were also obtained for the two ferrites at 147 °C.

The primary purpose of the paper is the investigation of the magnetic hyperfine interaction in compounds of iron which have spontaneous magnetic ordering. The isomer shift and quadrupole-splitting hyperfine interactions, which are also obtained from the Mössbauer spectrum, provide additional information on these compounds. The orthoferrites were chosen because they contain ferric ions on a single type of site with octahedral symmetry. This produces a simple six-line Mössbauer spectrum. The large number of compounds in this series made possible a study of the effect of the ionic radius of the rare-earth ion on the hyperfine interactions at the iron nucleus. The nickel ferrite,  $\text{NiFe}_2\text{O}_4$ , and magnetite,  $\text{Fe}_3\text{O}_4$ , represent more complicated situations. Both have the inverse-spinel-type structure, which contains ferric ions on sites with both tetrahedral and octa-

hedral symmetry. Although there are many other spinel-type ferrites, nickel ferrite and magnetite were selected because they are the only two in the series which are completely inverse. A completely inverse spinel has an equal number of ferric ions on the tetrahedral and octahedral sites. This equality simplifies the analysis of the Mössbauer spectrum because the intensities of the equivalent absorption lines for the two sites are equal if the recoilless fractions at the two sites are equal. The recoilless fractions at the tetrahedral and octahedral sites are nearly equal, and are considered equal for the purposes of this analysis. Nominally, magnetite may be considered to have the same structure as  $\text{NiFe}_2\text{O}_4$ , except that the  $\text{Ni}^{+2}$  ions on the octahedral sites are replaced with ferrous ions,  $\text{Fe}^{+2}$ . Since nickel ferrite contains ferric ions on two inequivalent sites, it produces two sets of six lines for a Mössbauer spectrum. Magnetite has ferric ions on both tetrahedral and octahedral sites and ferrous ions on octahedral sites; therefore, it would be expected to produce three sets of six lines each for the Mössbauer spectrum.

The isomer shift and hyperfine magnetic field are in a sense complementary parameters. The isomer shift is proportional to the total  $s$ -electron charge density at the nucleus, which is the sum of the spin-up  $s$ -electron density and the spin-down  $s$ -electron density; an increasing  $s$ -electron density is indicated by a decreasing isomer shift. The magnetic field is proportional to the spin density, which is the difference between the spin-up  $s$ -electron density and spin-down  $s$ -electron density. An increasing magnetic field indicates an increase in the net spin density at the nucleus. As a result, changes in the isomer shift or in the isomer shift differences between sites are not necessarily accompanied by corresponding changes in magnetic fields or differences in magnetic fields.

The magnetic fields are discussed in terms of Weiss molecular-field theory which relates the magnetization to the spin and the Curie or Néel temperature through the equation

$$\frac{M}{M_0} = B_s \left( \frac{3S}{S+1} \frac{M}{M_0} \frac{T_c}{T} \right), \quad (1)$$

where  $M$  and  $M_0$  are the magnetization and its saturation value,  $S$  is the spin,  $T_c$  is the Curie or Néel temperature, and  $B_s$  is the Brillouin function. It is generally assumed that the field  $H$  is proportional to  $M$  and thus has the same temperature dependence, so one writes

$$\frac{H}{H_0} = B_s \left( \frac{3S}{S+1} \frac{H}{H_0} \frac{T_c}{T} \right), \quad (2)$$

where  $H_0$  is the saturation field, and  $H$  is the ef-

fective field of the  $^{57}\text{Fe}$  nucleus.

The quadrupole splittings were calculated assuming an axially symmetric electric field gradient. For such a gradient which lies at an angle  $\theta$  to the direction of the magnetic field  $H$ , the energy levels of the excited state of  $^{57}\text{Fe}$  are given by

$$W_m = -\mu H m / I + (-1)^{l|m|+1/2} e^2 U_{zz}(0) \frac{1}{8} Q (3 \cos^2 \theta - 1), \quad (3)$$

where  $\mu = g I \mu_N$ , here  $g$  is the nuclear  $g$  factor,  $\mu_N$  is the nuclear magneton,  $U_{zz}(0)$  is the electric field gradient at the site of the nucleus along the  $z$  axis (along the  $H$  direction), and  $eQ$  is the nuclear quadrupole moment for a state with spin  $I$ . If  $\theta = \arccos(1/\sqrt{3})$ , the spectrum will be indistinguishable from one without quadrupole splitting. If the axially symmetric electric field gradient lies along the direction of  $H$ , Eq. (3) reduces to

$$W_m = -\mu H m / I + (-1)^{l|m|+1/2} e^2 U_{zz}(0) \frac{1}{4} Q. \quad (4)$$

If  $\theta$  is unknown, we can write the energy as

$$W_m = -\mu H m / I + (-1)^{l|m|+1/2} \frac{1}{2} \epsilon, \quad (5)$$

where  $\epsilon$  corresponds to the quadrupole splitting for a paramagnetic ion.

## II. ORTHOFERRITES

The four compounds  $\text{LaFeO}_3$ ,  $\text{PrFeO}_3$ ,  $\text{GdFeO}_3$ , and  $\text{TmFeO}_3$  were chosen in order to obtain representative values of the rare-earth ionic radius, which influences the properties of this series of compounds. For instance, the Néel temperature decreases as the ionic radius decreases. The ionic radius of the +3 oxidation state of the rare earth atoms decreases as the atomic number of the atom increases. These compounds all produce the six-line Mössbauer spectrum associated with a single ferric ion site in a magnetically ordered material.

The effect of pressure on the isomer shift of these compounds is given in Table I. All four orthoferrites have approximately equal isomer shifts at atmospheric pressure. Likewise, the isomer shifts all decrease by similar amounts with increasing pressure. This decrease in the isomer shift indicates an increase in the  $s$ -electron density

TABLE I. Isomer shifts for orthoferrites.

Pressure (kbar)	La	Pr	Gd	Tm
0	0.36	0.37	0.36	0.35
25	0.35	0.35	0.35	0.34
50	0.33	0.34	0.34	0.33
75	0.32	0.33	0.33	0.32
100	0.30	0.31	0.32	0.31
125	0.30	0.31	0.32	0.30
150	0.29	0.30	0.31	0.30
Relative to natural iron foil in mm/sec				

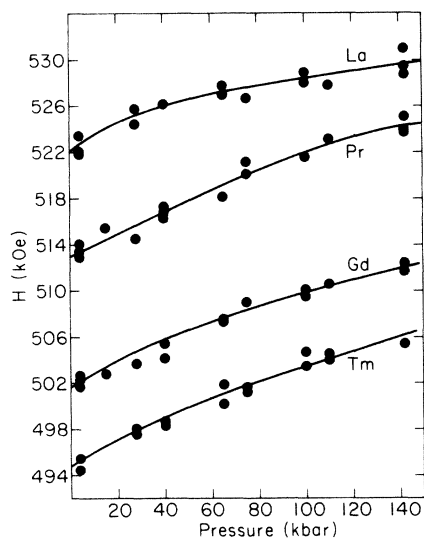


FIG. 1. Magnetic field vs pressure for four orthoferrites.

at the iron nucleus as the pressure is increased. This is the typical behavior of the high-spin ferric isomer shift for many other compounds. The decrease of the isomer shift with increasing pressure is due to the delocalization of the 3d orbitals, and the consequent reduction of the shielding of the 3s orbitals, which increases the 3s charge density at the nucleus.

The value of the magnetic field acting on the iron nucleus at atmospheric pressure ranges from 522 kOe for LaFeO<sub>3</sub> to 495 kOe for TmFeO<sub>3</sub>. This is consistent with the fact that LaFeO<sub>3</sub> has the highest Néel point at 740 °K and TmFeO<sub>3</sub> has the lowest at 632 °K.<sup>1</sup> The variation of the magnetic field with pressure for the four compounds is given in Fig. 1. The magnetic field increases with pressure for each compound, which is not an unexpected result. This implies an increase in the net spin density at the nucleus. We make the usual assumption that the magnetic field acting on the nucleus is proportional to the sublattice magnetization. The normal effect of pressure is to increase the sublattice magnetization due to a decrease in the interionic distance. Decreasing the distance increases the exchange integral and thus the Néel temperature increases. An increase in the Néel temperature increases the magnetization according to molecular-field theory.

The experimental magnetic field data can be used to calculate the Néel temperature for each compound as a function of pressure using the molecular field model. The values for the Néel temperature at atmospheric pressure are those given by Eibschütz *et al.*<sup>1</sup> Equation (2) is used with a value of  $S = 5/2$ . Given  $T/T_c$ , Eq. (2) is solved numerically for  $H/H_0$  on a digital computer using the

Newton-Raphson technique. The smoothed value at atmospheric pressure obtained from Fig. 1 is used to obtain  $H_0$ , which is assumed to be independent of pressure. Then the smoothed values of  $H$  are inserted along with  $H_0$  in Eq. (2). This is solved numerically to obtain the Néel temperature as a function of pressure. The results are presented in Fig. 2. The curve is linear for most of the pressure range for PrFeO<sub>3</sub>, GdFeO<sub>3</sub>, and TmFeO<sub>3</sub>.  $\partial T_c/\partial P$  has been shown to be linear for many compounds.<sup>8</sup> Thus the model employed seems reasonable for these three compounds. The curve for LaFeO<sub>3</sub> is nonlinear over a significant pressure range. It may be that the Néel temperature is actually changing in this manner for LaFeO<sub>3</sub>. However, the nonlinearity may indicate that the assumption that  $H_0$  was independent of pressure may be incorrect. (See discussion below for NiFe<sub>2</sub>O<sub>4</sub> and Fe<sub>3</sub>O<sub>4</sub>.) From Fig. 2 the following values for  $\partial T_c/\partial P$  (°K/kbar) are obtained: +0.73 for PrFeO<sub>3</sub>, +0.44 for GdFeO<sub>3</sub>, and +0.41 for TmFeO<sub>3</sub>. These values do not seem unreasonable in view of the values of  $\partial T_c/\partial P = +1.16$  for NiFe<sub>2</sub>O<sub>4</sub><sup>9</sup> and  $\partial T_c/\partial T = +2.05$  for Fe<sub>3</sub>O<sub>4</sub>.<sup>10</sup> As will be seen later in the paper, for NiFe<sub>2</sub>O<sub>4</sub> and Fe<sub>3</sub>O<sub>4</sub>,  $H_0$  at the octahedral site decreases by 10–20 kOe in 150 kbar. Such decreases may also occur for the orthoferrites and could radically effect  $T_c$ . For instance for Gd a decrease of 10 kOe in  $H_0$  when combined with the measured change in  $H$ , would give a value of  $\partial T_c/\partial P = 0.89$  °K/kbar.

The quadrupole splitting of the orthoferrites was obtained using Eq. (5). An axially symmetric electric field gradient which lies parallel to the magnetic field is normally assumed. The quantity

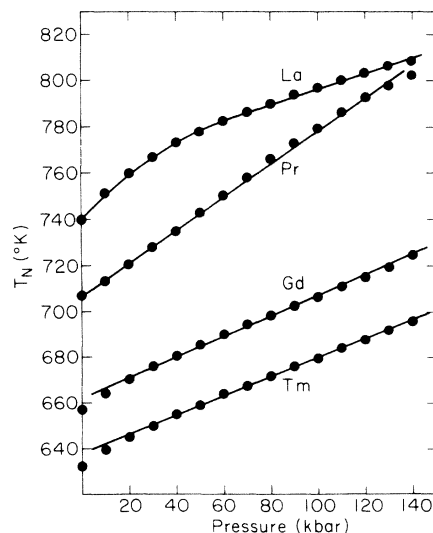


FIG. 2. Calculated Néel temperature vs pressure for four orthoferrites.

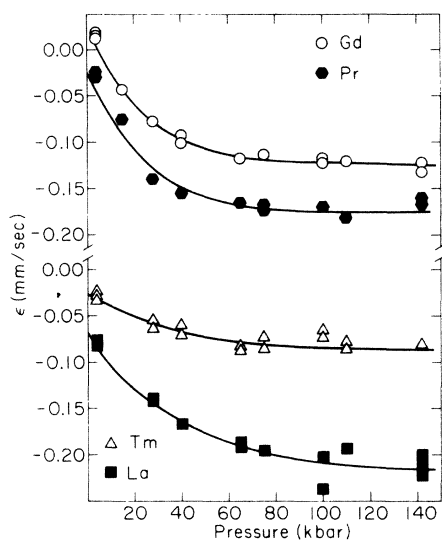


FIG. 3. Quadrupole splitting vs pressure for four orthoferrites.

used in analyzing the spectrum is  $\epsilon$ , which corresponds to the quadrupole splitting measured for a paramagnetic iron ion. Figure 3 shows the values

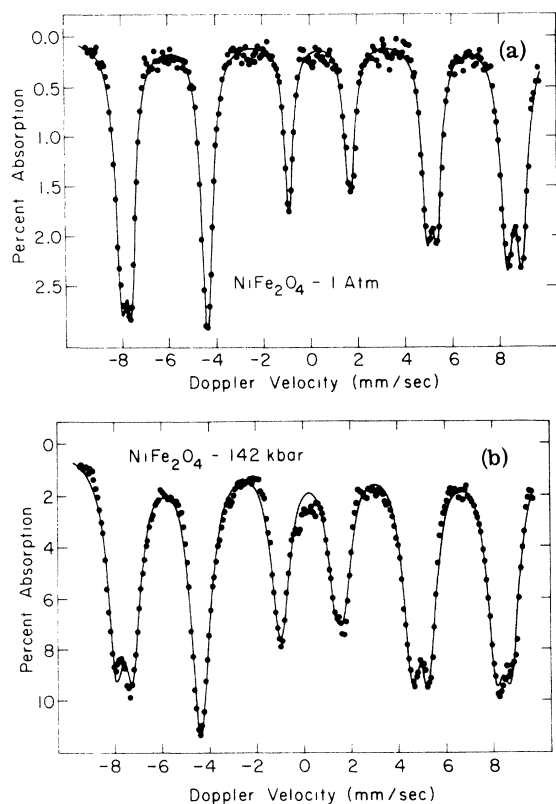


FIG. 4. (a) Atmospheric Mössbauer spectrum for  $\text{NiFe}_2\text{O}_4$  - 22°C, (b) Mössbauer spectrum for  $\text{NiFe}_2\text{O}_4$  at 142 kbar and 22°C.

of the quadrupole splitting for all four orthoferrites as a function of pressure. The ions in order of increasing atomic number (thus decreasing radius) are La, Pr, Gd, and Tm. At 140 kbar we see that the quadrupole splitting increases with increasing ionic radius. Apparently the larger rare-earth ions cause greater distortions about the iron ions as the lattice is compressed. Very small distortions of the oxygen ligands of the iron from octahedral symmetry are sufficient to account for even the largest quadrupole splitting observed at high pressure. Considering only the nearest oxygen neighbors, it can be shown that a relative change of about 1% in the iron-oxygen distance for two oxygen ions lying along one of the major octahedral axes produces the observed quadrupole splitting.

### III. NICKEL FERRITE

Nickel ferrite,  $\text{NiFe}_2\text{O}_4$ , is a completely inverse-spinel-type ferrite. There are equal amounts of ferric ions on the tetrahedral and octahedral symmetry sites. A typical atmospheric Mössbauer spectrum is shown in Fig. 4(a). Figure 4(b) shows a typical Mössbauer spectrum at 142 kbar. The Mössbauer spectra were analyzed assuming equal absorption areas for the tetrahedral and octahedral sites. High-pressure experiments were performed at both 22 and 147°C.

The effect of pressure on the isomer shifts of the tetrahedral and octahedral sites is given in Table II. The isomer shifts for both sites decrease with pressure, indicating an increase in the  $s$ -electron density at the nucleus. They are virtually independent of temperature. The isomer shift at the tetrahedral site is lower at one atmosphere than the octahedral isomer shift, and the tetrahedral isomer shift shows a larger decrease with pressure than the octahedral. While isomer shifts in compounds are complex functions of the bonding,<sup>9</sup>

TABLE II. Isomer shifts for nickel ferrite.

$T$ (°C)	Pressure (kbar)	Tetrahedral	Octahedral
22	0	0.24	0.35
	25	0.23	0.34
	50	0.21	0.33
	75	0.20	0.33
	100	0.19	0.32
	125	0.18	0.32
	150	0.18	0.31
147	0	0.23	0.34
	25	0.22	0.34
	50	0.21	0.33
	75	0.20	0.32
	100	0.19	0.32
	125	0.18	0.31
	150	0.18	0.31

Relative to natural iron foil in mm/sec

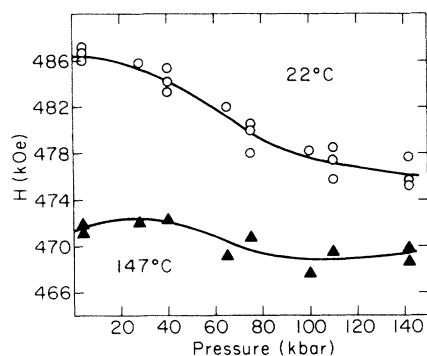


FIG. 5. Magnetic field vs pressure of  $\text{NiFe}_2\text{O}_4$  at tetrahedral site.

it has generally been assumed that the largest factor in decreasing isomer shift with increasing pressure is the delocalization of the  $3d$  orbitals and consequent decreased shielding of the  $3s$  electrons from the nucleus. This is consistent with the frequently observed decrease in the Racah (inter-electronic repulsion) parameters with increasing pressure.<sup>9</sup>

Figures 5 and 6 present the pressure dependence of the magnetic field at the tetrahedral and octahedral site, respectively, for both temperatures. The behavior of the two fields under pressure is quite different. The octahedral field is virtually unaffected by increasing pressure at room temperature and increases by approximately 8 kOe in 150 kbar at 147°C. The tetrahedral field, which is 35 kOe smaller than the octahedral at 1 atm and room temperature, decreases by 10 kOe in 150 kbar. On the other hand, at 147°C, the magnetic field is relatively constant for this latter site.

This behavior in nickel ferrite seems rather surprising in view of the simple behavior exhibited by the orthoferrites. The change in Néel tempera-

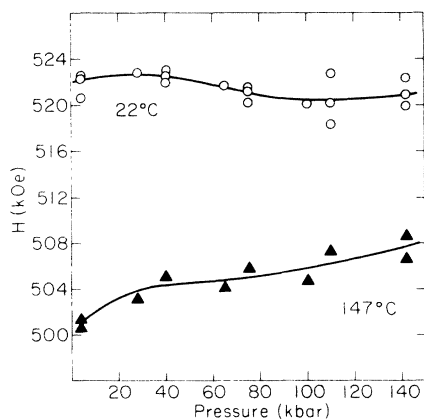


FIG. 6. Magnetic field vs pressure of  $\text{NiFe}_2\text{O}_4$  at octahedral site.

TABLE III. Magnetic fields calculated from Weiss theory for nickel ferrite.

$T$ (°C)	Pressure (kbar)	Octahedral	Tetrahedral
22	0	522	486
	25	523	488
	50	525	489
	75	527	490
	100	528	492
	125	529	493
147	150	530	494
	0	500	471
	25	504	475
	50	508	478
	75	511	482
	100	514	485
	125	517	487
	150	520	490

Given in kOe

ture with pressure for nickel ferrite has been measured by Foiles and Tomizuka.<sup>10</sup> Their measurements, which give a value of  $\partial T_c / \partial P = +1.16$  °K/kbar, were performed using strictly hydrostatic pressure, and consequently cover a pressure range of only 8 kbar. Samara and Giardini<sup>11</sup> have measured the Néel temperature of magnetite as a function of pressure up to 45 kbar and have found that it is linear over the entire region studied. We extrapolate the value for nickel ferrite linearly to the 150 kbar range as a first approximation for the purposes of these calculations. Using this value the Néel temperature is calculated for various pressures. Knowing the Néel temperature as a function of pressure enables us to calculate the expected magnetic field at each pressure. Equation (2) is employed with the assumption that  $H_0$ , the magnetic field acting on the iron nucleus at 0°K, is independent of pressure. We take the spin as  $S = 5/2$ . To obtain  $H_0$  for each site we use

TABLE IV. Changes in  $H_0$  calculated from Weiss theory for nickel ferrite.

$T$ (°C)	Pressure (kbar)	Tetrahedral	Octahedral
22	25	-2	-2
	50	-7	-4
	75	-11	-6
	100	-15	-8
	125	-17	-9
	150	-19	-10
147	25	-3	-1
	50	-8	-4
	75	-14	-7
	100	-17	-10
	125	-20	-12
	150	-22	-13

Given in kOe

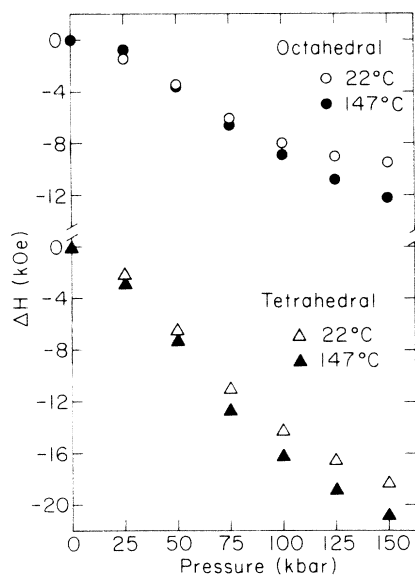


FIG. 7. Difference between experimental and calculated magnetic field vs pressure of  $\text{NiFe}_2\text{O}_4$ .

the atmospheric value of the magnetic field and take  $T_c = 889^\circ\text{K}$ .<sup>10</sup> Equation (2) is then solved for  $H$  at various pressures by inserting the proper value of  $T_c$  and solving the equation numerically on the computer. Calculated values for the magnetic field as a function of pressure are tabulated for both sites in Table III. These, of course, represent the expected field for an  $H_0$  independent of pressure. These calculated values for the magnetic field are subtracted from the smoothed experimental values and the difference  $\Delta H$  is shown in Fig. 7. It is noted that the experimental value for the field is always smaller than the calculated value. We can use Weiss field theory to calculate the change in  $H_0$  with pressure if we assume that the differences are totally due to changes in  $H_0$  with pressure.

TABLE V. Quadrupole splittings for nickel ferrite.

$T$ ( $^\circ\text{C}$ )	Pressure (kbar)	Tetrahedral	Octahedral
22	0	0.00	-0.02
	25	0.12	-0.04
	50	0.21	-0.06
	75	0.28	-0.06
	100	0.32	-0.05
	125	0.34	-0.03
	150	0.35	-0.02
147	0	0.01	-0.03
	25	0.11	-0.06
	50	0.19	-0.07
	75	0.24	-0.07
	100	0.28	-0.06
	125	0.29	-0.05
	150	0.30	-0.03

Given in mm/sec

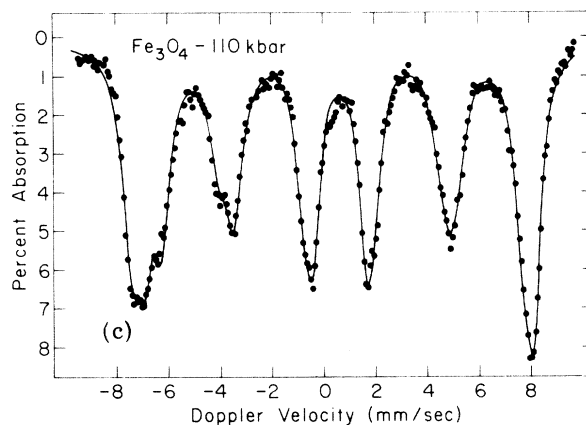
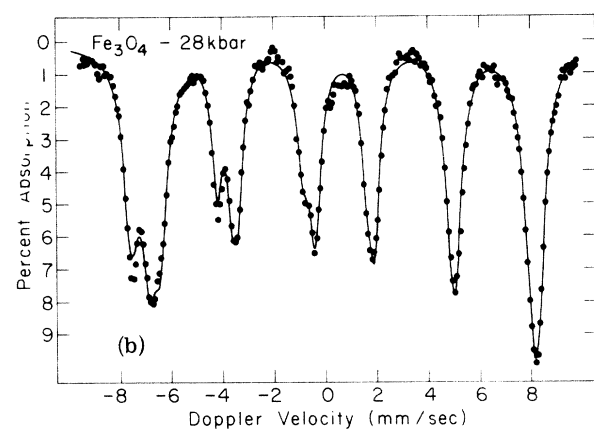
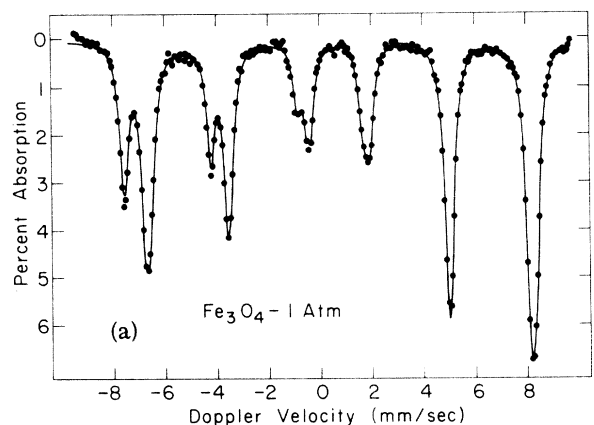


FIG. 8. (a) Mössbauer spectrum of  $\text{Fe}_3\text{O}_4$  and one atm and  $22^\circ\text{C}$ , (b) Mössbauer spectrum of  $\text{Fe}_3\text{O}_4$  at 28 kbar and  $22^\circ\text{C}$ , (c) Mössbauer spectrum of  $\text{Fe}_3\text{O}_4$  at 110 kbar and  $22^\circ\text{C}$ .

The Néel temperature as a function of pressure and the smoothed magnetic field as a function of pressure are known. Therefore, Eq. (2) is used to calculate  $H_0$  as a function of pressure using the previously mentioned numerical techniques. The values are listed in Table IV for both sites at both temperatures. The change in  $H_0$  at each site is independent of temperature within the experimental

accuracy, as it should be. This is evidence that it is reasonable to assume that  $H_0$  is changing with pressure. Note that the tetrahedral site has a larger change in  $H_0$  than the octahedral site.

The smoothed values of the quadrupole splitting for both sites are given in Table V. The quadrupole splitting at the octahedral site is very small for all pressures at both temperatures. Very small distortions are sufficient to give quadrupole splittings of this size, as we noted in the analysis of the orthoferrites. The behavior of the quadrupole splitting for the tetrahedral site is very similar for both temperatures. We can make a simple calculation for the tetrahedral site by considering only the nearest-neighbor oxygen ions to the iron. A change of 2% in the iron-oxygen distance of one of the oxygen ions relative to the others is sufficient to account for the largest observed splitting.

#### IV. MAGNETITE

Magnetite,  $\text{Fe}_3\text{O}_4$ , is a completely inverse-spinel-type ferrite with iron on two types of symmetry sites. The tetrahedral sites are totally occupied by ferric ions, and the octahedral sites are populated equally by ferrous and ferric ions. A typical atmospheric spectrum at room temperature is shown in Figure 8(a). At first glance the Mössbauer spectrum appears to consist of two fields at this pressure, with one having twice the area of the other. In the following discussion we show that this is not the best interpretation. Magnetite undergoes a change in conductivity at 120 °K. The conductivity increases by two orders of magnitude above this temperature, although it is still small compared to metals. There is a corresponding change in the Mössbauer spectrum. Below 120 °K the Mössbauer spectrum is quite complicated.<sup>12</sup> The explanation given by Verwey<sup>13</sup> is that above

120 °K there is a rapid hopping of an electron between the octahedral sites, so it is no longer correct to speak of ferrous and ferric octahedral ions. Below 120 °K the 3d electron apparently no longer hops, but is localized on one of the octahedral ions. Consequently, below 120 °K we can speak of ferric and ferrous ions. The conventional way to analyze the high temperature spectrum is to use two fields with one field having twice the area of the other.<sup>4,7</sup> Typical spectra for 28 kbar and 110 kbar at 22 °C are shown in Figs. 8(b) and 8(c). It is quite clear that three magnetic fields are present in the high pressure spectra. The Mössbauer spectra were analyzed assuming equal absorption areas for the three fields. It is impossible to obtain a satisfactory least-squares fit at the higher pressures using only two fields. The atmospheric-pressure spectra were also analyzed using a three-field fit. It was found that a smaller  $\chi^2$  was obtained for the three field analysis compared to the two field analysis. A reasonable explanation is available for these facts. There are two types of octahedral sites, which both have about the same size magnetic field but slightly different isomer shift at room temperature and 1 atm. These sites produce absorption lines which lie almost on top of one another. It appears as a single six-line spectrum of twice the area and larger linewidth than the tetrahedral site. The fact that the linewidth for the supposedly single octahedral field was larger than that of the tetrahedral was attributed to relaxation effects.<sup>14</sup> We find that as the pressure is increased the absorption lines of the two fields no longer coincide. Hereafter the three sites will be referred to as tetrahedral, octahedral 1, and octahedral 2. Octahedral 1 has a larger value of the magnetic field than octahedral 2. High-pressure experiments were performed at both 22 and 147 °C in order to obtain additional in-

TABLE VI. Isomer shifts for magnetite.

$T$ (°C)	Pressure (kbar)	Tetrahedral	Octahedral 1	Octahedral 2
22	0	0.27	0.54	0.76
	25	0.26	0.60	0.67
	50	0.26	0.61	0.62
	75	0.26	0.60	0.60
	100	0.27	0.58	0.58
	125	0.28	0.57	0.57
	150	0.28	0.56	0.56
147	0	0.27	0.61	0.67
	25	0.26	0.60	0.64
	50	0.25	0.60	0.62
	75	0.25	0.59	0.60
	100	0.25	0.59	0.59
	125	0.25	0.58	0.58
	150	0.26	0.56	0.56

Relative to natural iron foil in mm/sec

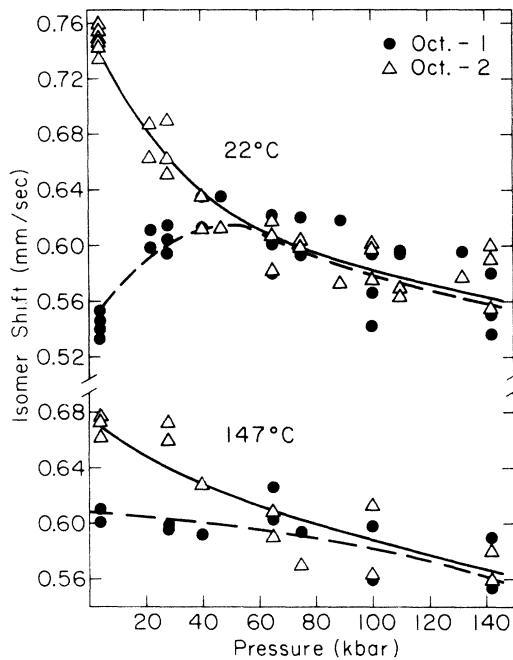


FIG. 9. Isomer shift vs pressure at octahedral sites in  $\text{Fe}_3\text{O}_4$ .

formation.

The pressure dependence of the isomer shift of all three sites is given in Table VI. The isomer shift at the tetrahedral site undergoes little change with pressure, and the values at both temperatures are approximately equal. The values of the tetrahedral isomer shift are typical for high-spin ferric. The isomer shift versus pressure for both types of octahedral site is shown in Fig. 9. Consider first the situation at  $22^\circ\text{C}$ . The two types of octahedral sites start out with significantly different isomer shifts. The octahedral-2 isomer shift decreases with the application of pressure and the octahedral-1 isomer shift increases until both have equal values at about 40 kbar. Then both isomer shifts decrease together with a further increase in pressure. At  $147^\circ\text{C}$  the isomer shifts of the two sites at 1 atm are much closer in value. Again they rapidly approach each other in value and then both decrease together with the further application of pressure. Recall that the isomer shift is proportional to the  $s$ -electron charge density at the nucleus, which is influenced by the  $3d$  electrons. These data show that there is not a perfect exchange of the  $3d$  electron between the two types of octahedral sites on the time scale of the Mössbauer experiment at low pressure, so that there is a higher probability of finding the  $3d$  electron on the nominally ferrous octahedral site than on the nominally ferric octahedral site at  $22^\circ\text{C}$ . At  $147^\circ\text{C}$  there is more thermal energy available,

which results in a more even distribution of  $3d$  electrons between the two sites. The application of pressure alters the energy levels of the two sites in such a way as to decrease the energy barrier between them. Eventually the charge densities appear identical for the two sites within the measurement time of the experiment. Then the decrease in isomer shift for both octahedral sites with a further increase in pressure indicates the delocalization of the  $3d$  electrons, which increases the  $s$ -electron density at the nucleus. Note that the observed isomer shifts for the two octahedral sites lie between the values of ferric and ferrous isomer shifts. High-spin ferric isomer shifts are normally about  $+0.35$  mm/sec and high-spin ferrous isomer shifts are normally significantly greater than  $1.0$  mm/sec relative to iron metal. The observed values indicate  $3d$  shielding greater than that of ferric, but less than that of ferrous. This is consistent with the idea of a relatively rapid electron exchange between a ferrous and ferric site.

The pressure dependence of the magnetic field at the tetrahedral site is given in Fig. 10. At room temperature it shows a rather large decrease with increasing pressure, whereas at  $147^\circ\text{C}$  it drops only slightly with pressure. The effect of pressure on the fields at both types of octahedral site is shown in Figs. 11 and 12. At room temperature the magnetic fields at the two octahedral sites are nearly equal, but they rapidly grow apart with pressure. The field at the octahedral-1 site undergoes an increase with pressure at  $22^\circ\text{C}$  and an even more rapid increase at  $147^\circ\text{C}$ . The octahedral-2 site's magnetic field, which undergoes a very large decrease with pressure at  $22^\circ\text{C}$ , remains approximately constant with pressure at  $147^\circ\text{C}$ .

We can apply the Weiss molecular-field model to magnetite in a manner similar to the analysis of nickel ferrite. Samara and Giardini<sup>10</sup> have mea-

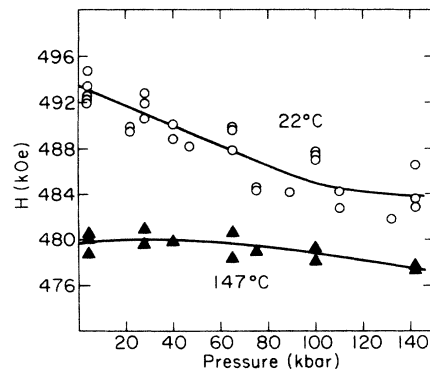


FIG. 10. Magnetic field vs pressure of  $\text{Fe}_3\text{O}_4$  at tetrahedral site.

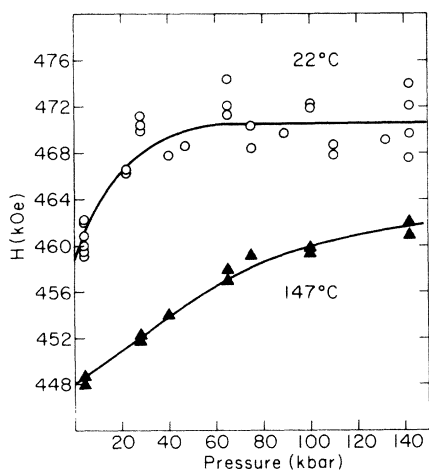


FIG. 11. Magnetic field vs pressure of  $\text{Fe}_3\text{O}_4$  at octahedral-1 site.

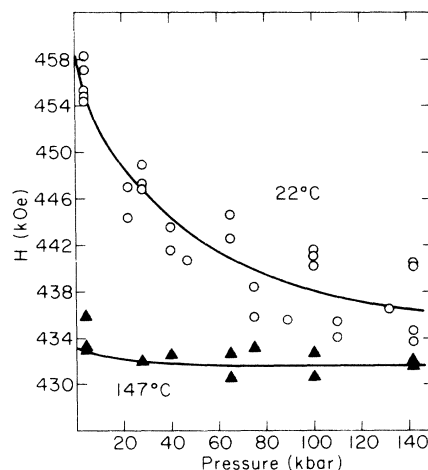


FIG. 12. Magnetic field vs pressure of  $\text{Fe}_3\text{O}_4$  at octahedral-2 site.

sured the Néel temperature of magnetite as a function of pressure up to 45 kbar and found that  $T_c$  increases linearly over this range with  $\partial T_c / \partial P = +2.05^\circ\text{K/kbar}$ . It seems a reasonable first approximation to extrapolate this value linearly to 150 kbar for the purposes of our calculations. As in the nickel ferrite analysis, we employ Eq. (2) with the assumption that  $H_0$  is independent of pressure. For the tetrahedral site we take  $S = 5/2$ . The value of  $B_s(T)$  does not vary greatly for small differences in the value of the spin  $S$ . For the octahedral sites we use  $S = 2.25$ , which is the average value of the ferrous and ferric spins.<sup>15,16</sup> As described previously, we calculate  $H$  as a function of pressure for all three sites assuming  $H_0$  is constant. The calculated values of  $H$  for all three sites at both temperatures are given in Table VII. These calculated values for the magnetic field are subtracted from the smoothed experimental values and the difference is shown in Fig. 13 for the tetrahedral field and Fig. 14 for the octahedral

fields. The behavior of the difference,  $\Delta H$ , for the tetrahedral site of  $\text{Fe}_3\text{O}_4$  is similar to that of  $\Delta H$  for nickel ferrite, as shown in Fig. 7. But  $\Delta H$  for the two octahedral sites in magnetite is different than  $\Delta H$  for the corresponding site in nickel ferrite and from each other. In magnetite there is a change in the  $s$ -electron charge density at each type of octahedral site, which may also effect the  $s$ -electron spin density at each site. We can try to eliminate this effect by taking the average of the differences for the two octahedral sites, i. e., by looking at the *average* change with pressure of the magnetic field at the two sites, and specifically, how this average field differs from the prediction

TABLE VII. Magnetic fields calculated from Weiss theory for magnetite.

$T$ ( $^\circ\text{C}$ )	Pressure (kbar)	Tetrahedral	Octahedral 1	Octahedral 2
22	0	493	458	458
	25	496	461	461
	50	499	464	464
	75	502	466	466
	100	503	467	467
	125	505	469	469
	150	506	470	470
147	0	479	448	433
	25	487	455	440
	50	494	461	446
	75	500	466	451
	100	504	471	455
	125	508	474	458
	150	512	477	461

Given in kOe

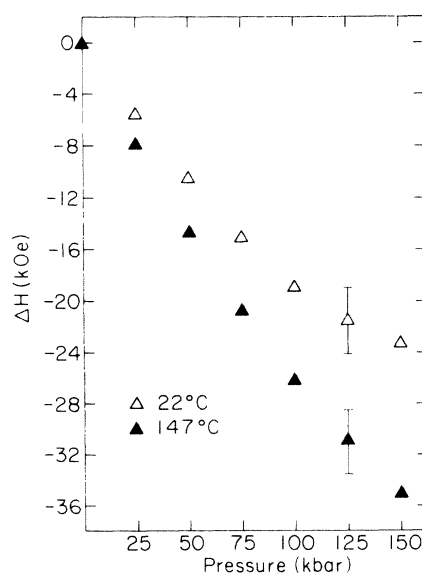


FIG. 13. Difference between measured and calculated magnetic field vs pressure of  $\text{Fe}_3\text{O}_4$  at tetrahedral site.

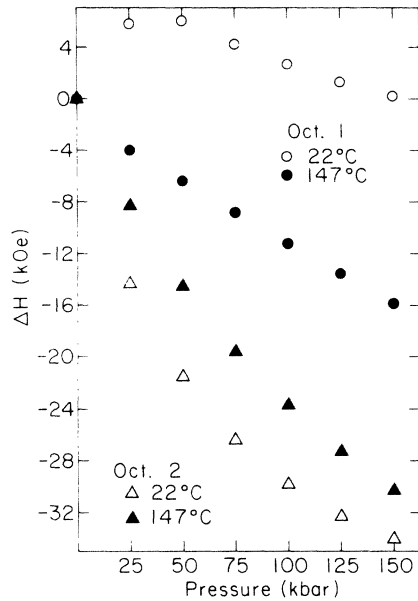


FIG. 14. Difference between measured and calculated magnetic field vs pressure of  $\text{Fe}_3\text{O}_4$  at octahedral sites.

of molecular-field theory, assuming  $H_0$  is not pressure dependent. This average difference is shown in Fig. 15. We note that the behavior of the average value is similar to that of the octahedral site for nickel ferrite, shown in Fig. 7. The difference  $\Delta H$  is greater for the tetrahedral site than for the octahedral in both magnetite and nickel ferrite. As in the previous analysis of nickel ferrite, we can use Weiss field theory to calculate the change in  $H_0$  with pressure if we assume that the differences are totally due to changes in  $H_0$ . The change in  $H_0$  with pressure is tabulated in Table VIII for all three sites. In addition, the average value of  $H_0$  for the two octahedral sites is shown in Table VIII. As previously mentioned, the change

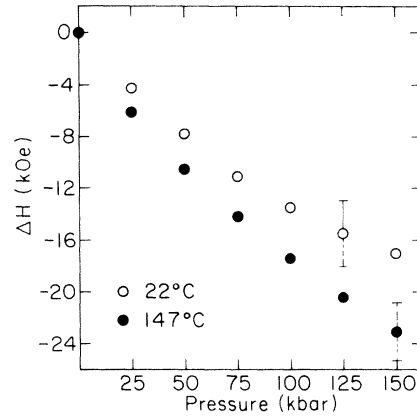


FIG. 15. Difference between the measured and calculated magnetic field vs pressure of  $\text{Fe}_3\text{O}_4$ ; averaged over the two octahedral sites.

in  $H_0$  with pressure should be independent of temperature in this model. The values for the average  $H_0$  for the two octahedral sites at both temperatures are probably the same within experimental error. The differences in  $H_0$  for the tetrahedral site at the two temperatures may be outside the experimental error. There may be other factors involved, but the predominant effect still seems to be the change in  $H_0$  with pressure.

As noted previously, we refer to the quantity  $\epsilon$  in Eq. (5) as the quadrupole splitting. The smoothed values of the quadrupole splitting for the three sites are given in Table IX. It is approximately independent of temperature at all three sites. All quadrupole splittings are small and are easily accounted for, as previously noted, by small distortions from ideal symmetry. For the tetrahedral site, a decrease of less than 2% in the iron-oxygen distance of one of the oxygen ions is sufficient to account for the observed high-pres-

TABLE VIII. Changes in  $H_0$  calculated from Weiss theory for magnetite.

$T$ ( $^{\circ}\text{C}$ )	Pressure (kbar)	Tetrahedral	Octahedral 1	Octahedral 2	Octahedral av.
22	25	-6	6	-15	-4
	50	-11	6	-22	-8
	75	-15	4	-27	-11
	100	-19	3	-30	-14
	125	-22	1	-33	-16
	150	-24	0	-35	-17
147	25	-9	-4	-9	-7
	50	-16	-7	-16	-11
	75	-22	-9	-21	-15
	100	-28	-12	-25	-19
	125	-33	-14	-29	-22
	150	-37	-17	-32	-24

Given in kOe

TABLE IX. Quadrupole splittings for magnetite.

T (°C)	Pressure (kbar)	Tetrahedral	Octahedral 1	Octahedral 2
22	0	0.02	0.00	0.01
	25	-0.12	-0.10	0.02
	50	-0.05	-0.17	0.05
	75	-0.07	-0.21	0.08
	100	-0.09	-0.23	0.10
	125	-0.11	-0.24	0.13
	150	-0.11	-0.24	0.14
147	0	0.01	0.02	-0.02
	25	-0.01	-0.05	-0.01
	50	-0.03	-0.11	0.01
	75	-0.06	-0.16	0.04
	100	-0.07	-0.18	0.06
	125	-0.09	-0.20	0.08
	150	-0.10	-0.20	0.09

Given in mm/sec

sure quadrupole splittings. A change of 1% in the iron-oxygen distance for two oxygen ions lying along one of the octahedron major axes produces the observed quadrupole splitting on the octahedral sites.

## ACKNOWLEDGMENT

The authors wish to acknowledge some earlier high-pressure work on  $\text{Fe}_3\text{O}_4$  in this laboratory by D. C. Grenoble, which was very helpful.

\*Work supported in part by the U. S. Atomic Energy Commission under Contract No. AT(11-1)-1198.

<sup>1</sup>M. Eibschütz, S. Shtrikman, and D. Treves, *Phys. Rev.* **156**, 562 (1967).

<sup>2</sup>J. Chappert and R. B. Frankel, *Phys. Rev. Lett.* **19**, 570 (1967).

<sup>3</sup>S. K. Banerjee, W. O'Reilly, and C. E. Johnson, *J. Appl. Phys.* **38**, 1289 (1967).

<sup>4</sup>F. van der Woude, G. A. Sawatzky, and A. H. Morrish, *Phys. Rev.* **167**, 533 (1968).

<sup>5</sup>P. Debrunner, R. W. Vaughan, A. R. Champion, J. Cohen, J. Moyzis, and H. G. Drickamer, *Rev. Sci. Instrum.* **37**, 1310 (1966).

<sup>6</sup>N. A. Halasa, Ph.D. thesis (University of Illinois, 1974) (unpublished).

<sup>7</sup>G. A. Sawatzky, F. van der Woude, and A. H. Morrish, *Phys. Rev.* **183**, 383 (1969).

<sup>8</sup>D. Bloch and A. S. Pavlovic, in *Advances in High Pres-*

*sure Research*, edited by R. S. Bradley (Academic, New York, 1969), Vol. 3.

<sup>9</sup>H. G. Drickamer and C. W. Frank, *Electronic Transitions and the High Pressure Chemistry and Physics of Solids* (Chapman and Hall, London, 1973).

<sup>10</sup>C. L. Foiles and C. T. Tomizuka, *J. Appl. Phys.* **36**, 3839 (1965).

<sup>11</sup>G. A. Samara and A. A. Giardini, *Phys. Rev.* **186**, 577 (1969).

<sup>12</sup>M. Rubinstein and D. W. Forester, *Solid State Commun.* **9**, 1675 (1971).

<sup>13</sup>E. J. Verwey and P. W. Haayman, *Physica (Utr.)* **8**, 979 (1971).

<sup>14</sup>W. Kundig and R. S. Hargrove, *Solid State Commun.* **7**, 223 (1969).

<sup>15</sup>E. Callen, *Phys. Rev.* **150**, 367 (1966).

<sup>16</sup>R. E. Mills, R. P. Keenan, and F. J. Milford, *Phys. Rev.* **145**, 704 (1966).